https://doi.org/10.5194/egusphere-2026-1405
Preprint. Discussion started: 1 April 2026

Integrating Muli-Step-Flux-Method for full range soil hydraulic characterisation: From saturation to oven-dryness

Mathilde B. S. Nielsen[1], Frederic Leuther[1], Efstathios Diamantopoulos[1]

[1]Chair of Soil Physics, University of Bayreuth, Bayreuth, 95447, Germany

Correspondence to: mathilde.nielsen@uni-bayreuth.de

Abstract. Soil hydraulic properties (SHP), defined by the water retention curve (WRC) and the hydraulic conductivity curve (HCC), are crucial to describe water storage and flow in soils. Several methods have been developed and combined to measure these two fundamental curves across the full range from saturation to oven dryness. However, for the HCC, there is still a data gap between approximately -1 to -100 hPa, which is expected to be affected by soil structure. We present an experimental workflow in which the multi-step-flux (MSF) method is integrated into the well-established combination of methods for measuring SHP, namely the falling head method, the simplified evaporation method, and the dew point method, specially designed to be applied to the same sample. The MSF is an adaptive, direct measurement of the HCC based on applying series of steady-state water flows to a soil sample characterised by unit hydraulic gradient. Once equilibrium is achieved, the sample is characterised at each step by a constant pressure head, constant water content and constant unsaturated hydraulic conductivity which is equal to the applied flux. We tested the method for three different soil columns: a repacked sand with a very well-defined air-entry pressure and two undisturbed structured silt loams. For the sand, the MSF results coincide with the saturated hydraulic conductivity value, measured with the falling head method. For the undisturbed loam samples, the structural effect on the HCC is clearly visible. Integrating the MSF into the common lab-workflow to characterise SHP will help future studies to investigate soil structure effect on SHP.

1 Introduction

The water retention curve (WRC) and the hydraulic conductivity curve (HCC) characterise the soil hydraulic properties (SHP). The WRC provides information on how much water is bound at specific energy levels within soils. The HCC describes how easily water flows through soil. A complete characterisation, from full saturation to oven-dry conditions, is essential for modelling water movement in soils and many related processes such as plant water uptake, nutrient transport, or pollutant leaching (Vereecken et al., 2016; Diamantopoulos et al., 2024).

Several methods have been developed to measure both curves accurately and reliably; however, none of them can measure both curves simultaneously from saturation to very dry conditions. Thus, a combination of methods is usually used in soil physical laboratories. A time-effective combination of methods consists of the simplified evaporation method (Wind, 1968; Peters and Durner, 2008), the dewpoint method (Schelle et al., 2013) and the falling head method for the saturated hydraulic

https://doi.org/10.5194/egusphere-2026-1405
Preprint. Discussion started: 1 April 2026

conductivity (Hohenbrink et al., 2023). For the WRC the simplified evaporation method can provide data points at pF -1-3, depending on how well the tensiometers are degassed. If the air-entry of the ceramic tip is used, an additional point at pF 3.8 (assuming that the air entry pressure of the tensiometer is around pF 3.8) can be obtained (Schindler et al., 2010). The dewpoint method provides WRC data between pf 4.5 and 6.5 (METER Group GmbH, 2025). For the HCC, the falling head method provides only one data point, the saturated hydraulic conductivity and the simplified evaporation method provides HCC points between pF 1.8 and 3 and one additional point at around pF 3.8 if the air-entry of the tensiometer is used (Schindler et al., 2010).

Therefore, in the HCC there are substantial data gaps in both the near-saturation (pF -1 to around 1.8) and dry (pF> 3.8) ranges. The latter has most recently been addressed by using humidity sensors, which extend the HCC curve to pF 5.5 for sand and pF 6 for loam (Bosse et al., 2025). The wet range data gab of the HCC has been bridged by Sarkar et al. (2019b) by adding an extra step to the falling head and simplified evaporation method. In this extra experiment, they applied a constant flux through the soil sample, by fixing the same negative pressure head at the top and at the bottom of the column. Under these conditions, gravity is driving water flow, and the flux density can be estimated by measuring the water outflow at the lower end of the column. By keeping equal and fixed the pressure heads at the top and at the bottom and by only changing the height of the soil column, different points of the HCC were estimated (Sarkar et al., 2019a, 2019b). A limitation of this method is that the porous plate on top of the soil has a smaller surface area than the soil, in order to allow air to invade the soil (for a drainage process). According to Sarkar et al. (2019a) this introduces an error of the flux rate to be less than 10%. A more robust method for directly measuring the near saturation unsaturated hydraulic conductivity, can be achieved by integrating the MSF method. In the MSF, water flow is maintained constant on top of the soil sample by drip irrigation, the pressure head is measured within the upper part of the soil sample, and the pressure head beneath the sample is regulated to ensure zero pressure head gradient in the sample or simple gravity only flow conditions (Weller et al., 2011). The advantage of the MSF is that the sample can freely ventilate without compromising the measurement.

Including the MSF as a standard measurement not only closes the data gab from saturation to field capacity, but it also provides the possibility to study structure driven macro-pore flow in detail (Jarvis et al., 2016). The near saturation data point of the HCC is known to be affected by soil structure which again can be examined by using the MSF (Bonetti et al., 2021).

A crucial point when comparing WRC and HCC from different methods is that the phenomenon of dynamic non-equilibrium must always be considered. In simple terms, dynamic non-equilibrium refers to the dependence of the measured WRC and HCC on the flow conditions (Hassanizadeh et al., 2002; Diamantopoulos and Durner, 2012; Vogel et al., 2023). Topp et al.(1967) were the first to show that, during a drainage process, more water is retained by the soil matrix (at a specific pressure head) under transient conditions compared with steady-state and equilibrium conditions. The faster the water flow, the greater the difference between transient and equilibrium WRC and HCC curves. Dynamic non-equilibrium effects are observed in both MSF measurements (Weller and Vogel, 2012) and simplified evaporation measurements (Diamantopoulos and Durner, 2012).

https://doi.org/10.5194/egusphere-2026-1405
Preprint. Discussion started: 1 April 2026

In this study, we present an experimental protocol that combines the falling head method, the MSF, the simplified evaporation method and the dew point method to characterise the WRC and the HCC including the pF range of -1 to 1.8. This measurement protocol is optimal for studies which examine soil structure effects on SHP. We applied the protocol to a repacked sand with a well-defined air-entry pressure to test the consistency of the different methods. In addition, two undisturbed samples of the same texture, collected under different soil tillage systems, allowed us to assess the protocol's ability to capture structural effects. To further evaluate the workflow and the importance of the MSF data, WRC and HCC models were fitted to experimental data with and without including the MSF data. For this, the single porosity van Genuchten-PDI model (Peters, 2013; Iden and Durner, 2014) was fitted to all the experimental data. For improving, the fitting for one of the silt loams samples, we had to introduce a bimodal version of the van Genuchten-PDI model that is more flexible in the wet range of the HCC.

2 Materials and Methods

2.1 Method workflow

Two undisturbed soil cores (volume of 250 cm^3 and a surface area of 50 cm^2) of the same texture (a silt loam (USDA, 1999)) were taken from a conventional ploughed topsoil with a bulk density of 1.5 g cm^{-3}(Loam 1) and from a subsoil under a disk harrow tillage system with a bulk density of 1.6 g cm^{-3} (Loam 2) by gently hammering a steel cylinder into the soil. In addition, four steel cylinders were repacked to a bulk density of 1.59 g cm^{-3}(standard error 0.01 g cm^{-3}) with a sand with uniform grain size distribution (Sand, Quarzsand, grain size distribution; >200µ 0.24%, >64µ 99.01%, <64µ 0.75%). All steel cylinders used in this study, had a hole (diameter 0.5 cm) at a depth of 2 cm from the top of the cylinder for the installation of a tensiometer for the MSF experiment. For all other experiments, the hole was sealed with vehicle body sealant (Teroson RB IX) and tape.

The workflow begins with a five-day stepwise saturation of the sample with degassed tap water. Four different methods were used in series for the sample to measure the WRC and HCC (Fig. 1): the falling head method (using the KSAT device, Meter Group USA), the multi-step flux method (using a custom made MSF device), the simplified evaporation method (using the HYPROP device, Meter Group USA), and the dew point method (using the WP4C device, Meter Group USA). After the MSF, a two-day stepwise re-saturation was conducted to ensure the sample was fully saturated and to reduce the risk of air entrapment for the HYPROP measurement. The experiment ends with the samples being dried in an oven at 105 °C for 24 hours. We repeated KSAT and HYPROP measurements for three sand columns to ensure reproducibility of the repacking and SHP, and for the MSF we used one sand column, which was not used for other experiments. Both undisturbed loam columns completed the full workflow.

https://doi.org/10.5194/egusphere-2026-1405
Preprint. Discussion started: 1 April 2026

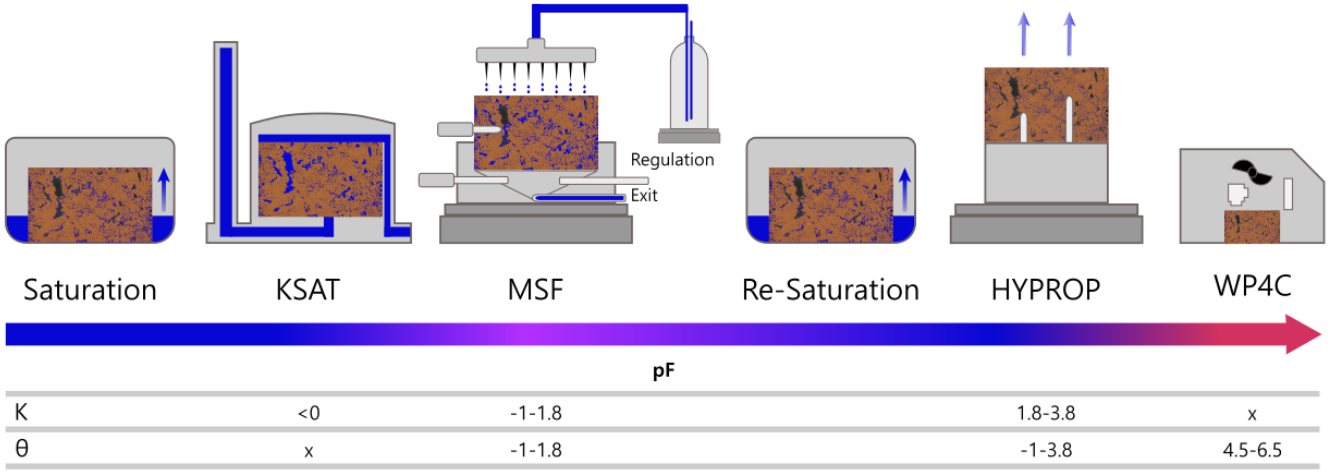

Figure 1: A schematic overview of the workflow.

2.1.1 Falling head, KSAT

The saturated hydraulic conductivity (K_{sat}) was measured using the falling head method as implemented in the KSAT device. The flux density at saturation for laminar flow is described by on Darcy's law Eq. (1):

$$q = -K_{sat}\nabla H \quad (1)$$

Where q is the flux density [cm day^{-1}], H is the hydraulic head [cm], defined as: $H = h + z$, where z is the spatial coordinate [cm] and h is the pressure head [cm], and K_{sat} [cm day^{-1}] is the saturated hydraulic conductivity. The falling head method works by mounting a fully saturated soil sample on the KSAT device, which consists of a water reservoir with a defined volume. Once the experiment starts, the water moves from the container and through the sample. A pressure sensor continuously measures the pressure drop between the free surface of water in the container and the upper end of the sample (outflow point). An exponential decay function is automatically fitted to the measured data and the K_{sat} value is estimated as a function of the fitted exponent. For more information about the method, we refer to Operation Manual (METER Group GmbH).

2.1.2 Multistep flux, MSF

The MSF quantifies the hydraulic conductivity near saturation (pF -1 to 1.8). Water flow during an MSF experiment is described by Darcy-Buckingham's equation:

$$q = -K(h)\nabla H \quad (2)$$

where h is the pressure head [cm], and K(h) is the unsaturated hydraulic conductivity [cm day^{-1}] at h. For the MSF method, a constant q is applied on top of the soil column, and the h is measured with a tensiometer at 2 cm. At the bottom of the column,

https://doi.org/10.5194/egusphere-2026-1405
Preprint. Discussion started: 1 April 2026

the same pressure head, h, is applied, forcing the system to reach unit hydraulic heat (gravity flow), where the whole column is characterised by a unique water flux q, pressure head h and water content. Under these conditions, equation (2) becomes:

$$q = -K(h) \quad (3)$$

And the applied flux is equal to the unsaturated hydraulic conductivity at pressure head, h.

The MSF device consist of a Mariotte bottle, a system of tubs, a peristaltic pump, an irrigation head, two balances, a tensiometer installed inside the sample, a sample chamber, a pressure sensor installed in the chamber, two pressure-regulation valves, a vacuum pump, and custom-made regulation and logging software (LabVIEW). Prior to the start of the experiment, a three-point calibration curve of the tensiometer was established using a hanging water column. The calibration curve was then used to correct the tension measurements at the data processing stage. The pressure sensor, connected to the chamber below the sample, was checked against a high-precision reference sensor. After the calibration phase, each soil sample is mounted on a pressure plate (ROBU VitraPOR Filterplatte biplane ø 90mm, por. ASTM Fine) fixed in the chamber, with a tensiometer installed in the sample (2 cm). Water flow is supplied by a Mariotte bottle and distributed through a peristaltic pump and an irrigation head over the sample. Both the sample and the Mariotte bottle were placed on an electronic balance to calculate water flux and changes in the samples water content. Given the accuracy of the balances, we estimate that the error of the water content of the sample is 0.3%. The chamber under the sample is connected to the water outflow, a pressure sensor and a regulation system (Fig. 1). The regulation system is automatically adjusting the pressure head at the bottom of the sample to the one measured by the tensiometer inside the soil sample. This is done by two regulating valves and by opening to either under pressure or atmospheric air. The maximum difference between measured and adjusted potential was controlled by a software input parameter, the delta value, which introduces an uncertainty of the final pressure head. At low pressure head (0 to -5 cm), the delta values were set between 1.5-2, for pressure head values between -5 and -10 cm, between 2-3, and for <-10 cm, between 2-4.

Different water fluxes were applied on the soil sample in a stepwise manner, starting with a high flow rate and then gradually reducing the flow rate for each new step (drainage process). Each step run for at least one hour to ensure that the system reaches steady state water flow conditions and equilibrium conditions were assessed for each sample by checking when the matric potential and sample mass remained relatively stable. Once the experiment was finished, the actual flow rates were calculated from the changes in the Mariotte bottle's weight during the last 10 minutes of the step. For the tension, we use the median of the tension over the last 10 minutes of each step.

To further evaluate the agreement between the simplified evaporation method and the MSF, the water content for each flux can also be calculated by:

https://doi.org/10.5194/egusphere-2026-1405
Preprint. Discussion started: 1 April 2026

$$\theta_i = \frac{(\theta_{i-1} * V_{total} + \frac{d_i}{\rho_w})}{V_{total}} \quad (4)$$

where θ_i is the volumetric water content at flow rate step i [$cm^3\ cm^{-3}$], V_{total} is the total volume of the sample (250 cm^3), ρ_w is the water density assumed equal to 1 g cm^{-3} for all calculations and d_i is the weight difference from step i and step i-1 [g]. Critical to this calculation is the assumption that the initial water content θ_0 [$cm^3\ cm^{-3}$] is given by:

$$\theta_0 = \theta_{sat} = n \quad (5)$$

where n [$cm^3\ cm^{-3}$] is the estimated porosity from:

$$n = 1 - \frac{\rho_b}{\rho_s} \quad (6)$$

Where ρ_b is the bulk soil density and ρ_s is the density of the particle (2.65 g cm^{-3}).

2.1.3 Simplified evaporation method, HYPROP

After re-saturation, the WRC (pF -1–3.8) and HCC (pF around 1.8–3.8) were estimated using the HYPROP device. Two tensiometers were installed at 1.25 cm and 3.75 cm inside the sample and the whole setup was placed on an electronic balance connected to a computer. The sample let evaporate until air entered both tensiometers.

The data points on the WRC were calculated by averaging the pressure head values measured by two tensiometers and the weight loss measured by the electronic balance. Data points on the HCC were estimated by applying darcy law to the weight and tensiometer data (Peters and Durner, 2008).

2.1.4 Dew point, WP4C

Subsamples of around 3 grams were taken from the top, middle and bottom of each soil column at the end of the HYPROP experiment to cover a broad range of pressure heads between pF 4.5 and 6.5. First, the weight of the moist sample was quantified. Second, pressure head of the dry sample was measured using WP4C device. Third, the subsamples and HYPROP samples were oven dried at 105 °C for at least 24 hours to calculate the gravimetric water content, the total soil dry weight and bulk density. The gravimetric water content of the subsamples is finally converted to volumetric water content by using the bulk density.

2.2 SHP models and fitting strategy

2.2.1 SHP models

To evaluate our data, two SHP models were fitted. The first model is the van Genuchten-PDI model (VG-PDI) (Peters, 2013; Iden and Durner, 2014) which is given by:

$$\theta(h) = (\theta_s - \theta_r)S^{cap} + \theta_r S^{ad} \quad (7)$$

https://doi.org/10.5194/egusphere-2026-1405
Preprint. Discussion started: 1 April 2026

where θ(h) is the volumetric water content [$cm^3\ cm^{-3}$] at pressure head h [cm], θ_s is the saturated water content [$cm^3\ cm^{-3}$], θ_r is the maximum water content for the water adsorption part [$cm^3\ cm^{-3}$], S^{cap} is the saturation function for the capillary part, and S^{ad} is the saturation function for the adsorptive part (Peters, 2013; Iden and Durner, 2014).

The HCC for the VG-PDI model is:

$$K(h) = K_{sat}[(1-\omega)K_{rel}^{cap}(S^{cap}) + \omega K_{rel}^{film}(S^{cap})] \quad (8)$$

where K_{sat} is the saturated hydraulic conductivity [cm day^{-1}], K_{rel}^{cap} is the relative conductivity for the capillary part and K_{rel}^{film} is the relative conductivity for the adsorptive (film) part, and ω is a weighting factor. For more information about the model, the reader is referred to Peters (2013) and Iden and Durner (2014).

Since the VG-PDI model couldn't fully describe the Loam 2 data, we made a slight modification by adding a macropore conductivity component in the HCC. In that case:

$$K(h)_{total} = K(h)_{mac} + K(h)_{matrix} \quad (9)$$

Where $K(h)_{total}$ is the full model, $K(h)_{mac}$ describes the macropore region as one single S-sharp:

$$K(h)_{mac} = K_{sat_{mac}} * (1 + (\alpha_{mac} * |h|)^{n_{mac}})^{m_{mac}} \quad (10)$$

where $K_{sat_{mac}}$ is the hydraulic conductivity at saturation for the macropore region, which is defined by equation (13), and α_{mac}, n_{mac}, and m_{mac} (m_{mac}= 1-1/n_{mac}) are fitting parameters that reflect the shape and steepness of the S-shape. $K(h)_{matrix}$ in equation (9) describes the matrix component of the model that fits the MSF and HYPROP data. $K(h)_{matrix}$ is described by van Genuchten-PDI following equation (8).

$$K(h)_{matrix} = K_{sat_{matrix}} * \left((1-\omega)K_{rel}^{cap}(S^{cap}) + \omega K_{rel}^{film} * (S^{cap})\right) \quad (11)$$

where $K_{sat_{matrix}}$ is the hydraulic conductivity at saturation for the matrix region, determined by fitting.

We note that the K_{sat} value measured with the falling head method is assumed to be equal to:

$$K_{sat}^{falling\ head} = K_{sat_{mac}} + K_{sat_{matrix}} \quad (12)$$

2.2.2 Fitting strategy

Data for each soil and method were compiled using the LABROS SoilView analysis software (5.4.0.0), which further enabled the fitting of the WRC and HCC described in the previous paragraph. For all the fittings presented in the results section, the following weights were given to the different data groups: i) for HYPROP and WP4C data, a weight of 1 was used and for ii) KSAT and MSF data, a weight of 10 was used. The different weighting scheme was implemented to account for the higher number of HYPROP and WP4C data points relative to the MSF (and KSAT) data. For all three soils we conducted two fittings. In the first fitting (VG-PDI without MSF data) the K_{sat} was fixed to the measured value, and the MSF data were omitted from

https://doi.org/10.5194/egusphere-2026-1405
Preprint. Discussion started: 1 April 2026

the objective function. In the second fitting (VG-PDI with MSF data) the K_{sat} was fixed to the measured value, and the MSF data were included in the objective function.

Only for the Loam 2 soil sample, we additionally fitted the model described by equations (9)-(12). First, we fitted the VG-PDI model to the HYPROP, MSF, and WP4C data (excluding K_{sat}). In that way, the "matrix" SHP were estimated and described by the VG-PDI model, where the hydraulic conductivity $K_{sat_{matrix}}$ where fitted. Afterwards, we calculate the $K_{sat_{mac}}$ by:

$$K_{sat_{mac}} = K_{sat}^{falling\ head} - K_{sat_{matrix}} \quad (13)$$

And applied equation (10) for the HCC, by assuming n_{mac}=10 [-], α_{mac}=4 [cm^{-1}] (big pores).

3 Results and Discussion

3.1 Result of the repacked sand: proof of the workflow

For the repacked sand, the combination of methods provided a full data set of the WRC from approximately pF 0 to pF 6.5 and for the HCC from pF -1 (assumed to correspond to the pF for K_{sat}) to pF 2.5 (Fig. 2, left panel). The sand had a well-defined air-entry value at around pF 2 after which a steep drop of water content from 40 to 5 vol.% occurred. The calculated water retention data from the MSF were 42 vol.% at pF 0.54, 39.7 vol.% at pF 0.57, 38.6 vol.% at pF 0.59, and 28.9 vol.% at pF 1.72, which were very close to the water retention estimated with HYPROP (41.1-38.6 vol.%). Differences can be explained by (i) the higher uncertainty due to tubing and the accuracy of the balance and (ii) the flow rate dependence of the SHP (Diamantopoulos and Durner, 2012; Diamantopoulos et al., 2015). In the simplified evaporation method, the samples are evaporating continuously, which is a slow but dynamic process. In the MSF, we waited for some time for the system to reach equilibrium in water flow, water content and pressure head. According to Diamantopoulos and Durner (2012), in equilibrium, less water is retained by the soil at a specific pF value compared to the dynamic experiment, which can explain why the MSF data show a lower water content than the simplified evaporation data. The water contents derived by WP4C were between 1.95-0.03 vol.% and showed good agreement with the HYPROP data.

The log-transformed saturated hydraulic conductivity, $\log_{10}(K_{sat})$, for the sand was 2.83 $\log_{10}$(cm day^{-1}) (standard error 1.72) (Fig. 2, left lower panel). The log-transformed conductivity, $\log_{10}(K(h))$, measured with the MSF ranged from 2.91-2.80 $\log_{10}$(cm day^{-1}) for the pF range of 0.5 to 1.9. The HYPROP $\log_{10}(K(h))$ data for the sand were in the range -1.08-(-4.11) $\log_{10}$(cm day^{-1}) at pF 2-2.5.

Overall, the agreement of hydraulic conductivity data and the water retention data measured with the KSAT, the MSF, and the HYPROP device (Fig. 2 lower panel) was excellent, indicating good consistency between methods and confirming the reliability of the measurements across the investigated pressure head range. This is particularly important because this combination of methods has the potential to characterize near-saturation unsaturated hydraulic conductivity, which is currently not captured by state-of-the-art methods (Hohenbrink et al., 2023) and pedotransfer functions (Weber et al., 2024).

https://doi.org/10.5194/egusphere-2026-1405
Preprint. Discussion started: 1 April 2026

3.2 Result of the undisturbed loams; the workflows ability to measurer structural effects in SHP

It has been suggested that soil structure affects the SHP near saturation (Bonetti et al., 2021). The WRC for the two loams had similar shapes, except that Loam 1 begins at a higher water content and had a small step drop in the wet range (around pF 1), whereas Loam 2 decreases more steadily (Fig. 2 upper middle and right panel). The HYPROP WRC data range for Loam 1 was 44-23 vol.%, and for Loam 2 it was 39-20 vol.%. The MSF water retention data for Loam 1 ranged from 44-37 vol.% water content, corresponding to a pF range of 0.4-1.1. Thereby the MSF captured the small step decrease at around pF 1 which was also observed in the HYPROP data, thereby increasing confidence in the reliability of the MSF. For Loam 2, the ranges were 39.5-38.8 vol.% water content and pF range of -0.2-0.6. For both loams, the MSF data displayed lower water content at the same pF values compared to the HYPROP data, as also observed for the sand. We again attributed this to differences in the dynamic and equilibrium states of the two methods. The WP4C data for Loam 1 ranged from 14-2 vol.% water content, corresponding to a pF range of 4.4-6.4, and for Loam 2, from 14.4-3.4 vol.% water content, with a pF range of 4.3-6. For both loams, the WP4C data continued from the HYPROP measurements, demonstrating good agreement between the two methods. For the Loam 1, there was a smooth transition from the $\log_{10}(K_{sat})$ measurement (2.55 $\log_{10}$(cm day^{-1})) to the $\log_{10}K(h)$ MSF data (1.74-(-0.24) $\log_{10}$(cm day^{-1})) and then to the $\log_{10}K(h)$ HYPROP measurements (-3.1-(-4.08) $\log_{10}$(cm day^{-1})) (Fig. 2 lower middle). For Loam 2, there was a 2 order of magnitude drop from the $\log_{10}(K_{sat})$ measurement (3.09 $\log_{10}$(cm day^{-1})) compared with the $\log_{10}K(h)$ MSF data points (0.99-0.46 $\log_{10}$(cm day^{-1})). The $\log_{10}K(h)$ HYPROP measurements (-0.68-(-4.15) $\log_{10}$(cm day^{-1})) smoothly continued the $\log_{10}K(h)$ MSF data (Fig. 2 right panel).

Both loams had no clear air-entry. The most notable difference between the two loams was observed for the MSF data: Loam 1 conducted more water than Loam 2 at the same pF in the range near saturation (Fig. 2), indicating differences in the structural pore sizes. Loam 1 originated from a topsoil plot where the main structure-forming processes were ploughing (Schlüter et al., 2018; Munkholm et al., 2013), freeze-thaw cycles (Leuther and Schlüter, 2021), and biological activity (Meurer et al., 2020). Loam 2, in contrast, was a subsoil with no tillage, and presumably, no freeze-thaw events; its main structural-forming processes were likely earthworm and plant root activity (Zhang et al., 2018), as well as compression from the overlying layer. Therefore, we suspect that Loam 1 contains more medium-sized pores, created by tillage, compared to Loam 2. Combining knowledge of the soil's origin with the HCC data, we can conclude that the two loams have distinctly different soil structures.

https://doi.org/10.5194/egusphere-2026-1405
Preprint. Discussion started: 1 April 2026

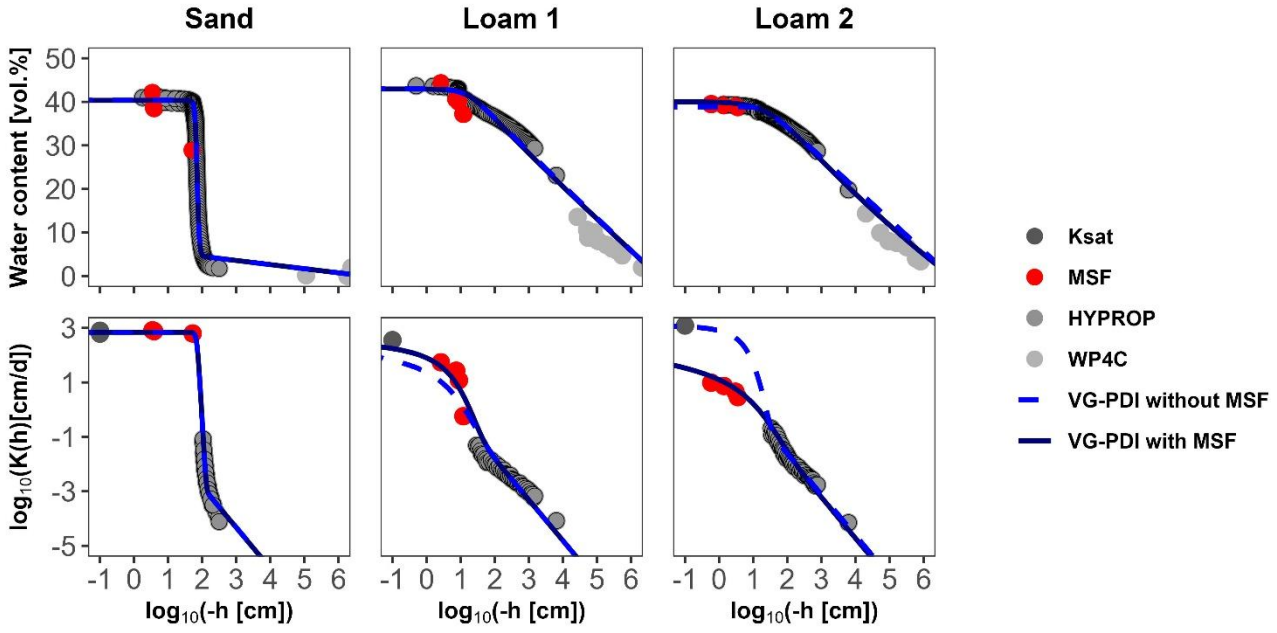

Figure 2: Water retention data and WRC on the top panel for the three soils. Bottom panel data of hydraulic conductivity data and HHC. For the saturated hydraulic conductivity matrix potential is not measured but set to be -1 $\log_{10}$(-h[cm]) The sand has three replicas for the KSAT and HYPROP devices.

3.3 The model

SHP models are frequently used in soil physics and soil hydrology studies to simulate soil water dynamics with the Richards equation (Richards, 1931), with dual-permeability models (Holbak et al., 2021), to develop pedotransfer functions (Weber et al., 2024), and to calculate the equivalent pore-size distribution (Leij et al., 2002), among other applications.

For all samples, the WRC models provided good fits to the data. For the sand HCC, VG-PDI fits with and without MSF data agreed very well, even when the MSF data were not included in the objective function (RMSEs 0.17 and 0.18 respectively) (Fig. 2, left). Therefore, for an unstructured, repacked soil with a very well-defined air entry pressure, the combination of KSAT, HYPROP, and WP4C, measurements cover most of the SHP range and inclusion of MSF data does not necessarily improve the fit.

For Loam 1, both VG-PDI HCC fittings (with and without MSF data) captured the data reasonably well (RMSEs 0.38 and 0.36 respectively). However, the VG-PDI without MSF data showed a slightly poorer fit (Fig. 2, middle panel) to the MSF data, underestimating the HCC at the wet range (around pF 1), while the fits were nearly identical for the rest of the pF range. A clear difference was observed for the HCC of Loam 2 between the VG-PDI without MSF and VG-PDI with MSF data (RMSEs 0.54 and 0.23 respectively) (Fig. 2, right). The VG-PDI without the MSF data overestimated the near saturation

https://doi.org/10.5194/egusphere-2026-1405
Preprint. Discussion started: 1 April 2026

unsaturated hydraulic conductivity compared with the measured MSF data. The VG-PDI with MSF data cannot describe both the K_{sat} at pF -1 and the MSF data. Even though the K_{sat} was fixed to the measured value, the VG-PDI model predicted an unrealistic drop of the conductivity near saturation, something that cannot be justified physically (Ippisch et al., 2006). To adequately describe these data, a different type of model is required to represent the behaviour mathematically. As described in Section 2.2, this issue was addressed by adopting a model that combines an extra van Genuchten (1980) S-shaped function, to describe the drop in the conductivity in the wet range (Fig. 3). Only with this approach could the full HCC range be satisfactorily described. These results indicate that soil structure strongly affects the HCC, a feature not evident in the WRC data. This simple extension of the van Genuchten-PDI model is not meant to be the solution for modelling these kinds of data, but it highlights the need for a new modelling approach to represent this hydraulic behaviour because a small volume of water contained in large pores drives the sharp decline in the hydraulic conductivity curve. Recognizing these structural effects on near-saturation conductivity, and the consequent need to modify existing models, would not have been possible without incorporating MSF measurements into the SHP workflow.

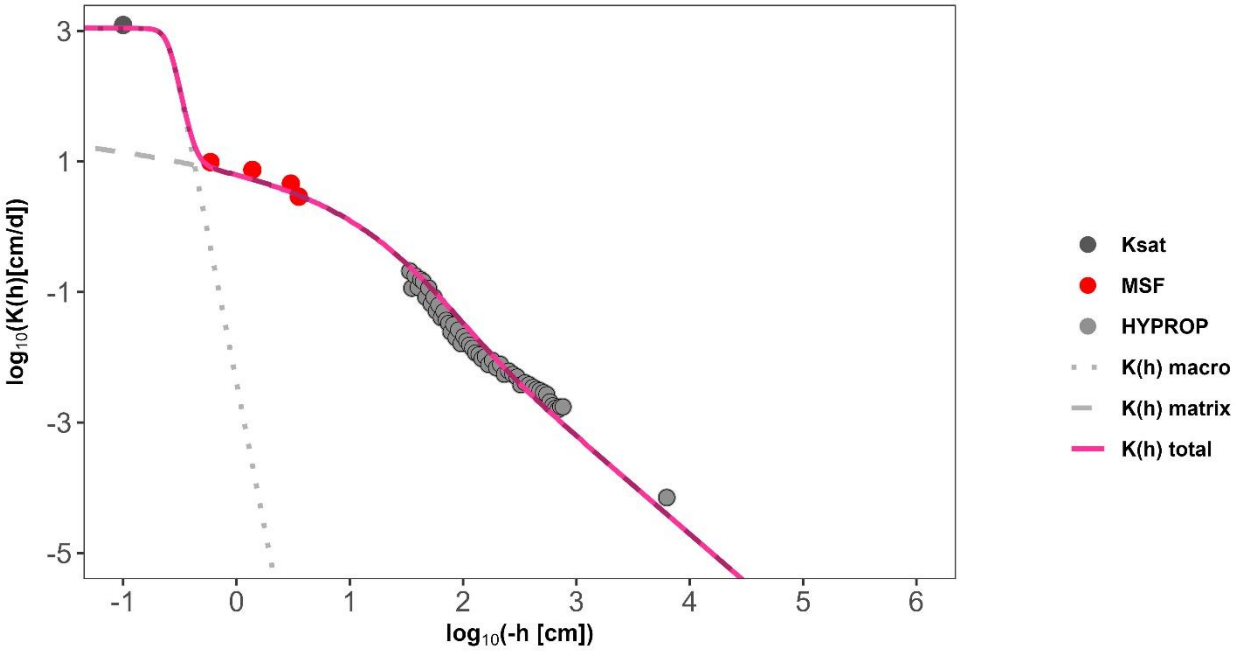

Figure 3: The modified model, $K(h)_{total}$, for HCC that can capture both the K_{sat} and the MSF for Loam 2, and the two compartments of the $K(h)_{total}$ model the $K(h)_{macro}$ and $K(h)_{matrix}$.

4 Conclusions

In this study, we present a workflow for measuring SHP from saturation down to pF 6.5 for the WRC and to approximately pF 3.8 for the HCC, including the critically important range between pF -1 and 1.8, which is highly dependent on soil structure. We demonstrate that the MSF is a reliable method that can be integrated with existing techniques. Our findings shows that the

https://doi.org/10.5194/egusphere-2026-1405
Preprint. Discussion started: 1 April 2026

absence of near-saturation HCC data, as measured by the MSF, can cause overestimation of hydraulic conductivity close to saturation during modelling. Furthermore, for structurally complex soils, new models may be required to adequately describe SHP mathematically. Lastly, the new protocol can be used to characterise structural pore domains like in dual-permeability model, but additional studies are needed in that direction.

Code/Data availability

Code and data not available.

Author contribution

Mathilde B. S. Nielsen: conceptualization, data curation, formal analysis, visualization, writing original draft and editing. Frederic Leuther: conceptualization, supervision, writing - review and editing. Efstathios Diamantopoulos: conceptualization, supervision, writing - review and editing.

Competing interests

The authors have no competing interests.

Acknowledgments

We would like to thank the University of Bayreuth for funding the position of Mathilde B. S. Nielsen. Andreas Kolb, and the University of Bayreuth's electronic workshop for technical support in building and optimizing the MSF. We also thank Hans Jörg Vogel for providing hardware for the MSF and Florian Ebertseder from the Bayerische Landesanstalt für Landwirtschaft for allowing us to collect the undisturbed samples. Additionally, we acknowledge the use of the software Grammarly to improve spelling, grammar, and sentence structure. This research was co-funded by the European Union under the project Path4Med (grant number 101156867), https://www.path4med.eu/ (accessed on 10 November 2025), https://cordis.europa.eu/project/id/101156867

References

Bonetti, S., Wei, Z., and Or, D.: A framework for quantifying hydrologic effects of soil structure across scales, Commun Earth Environ, 2, https://doi.org/10.1038/s43247-021-00180-0, 2021.

https://doi.org/10.5194/egusphere-2026-1405
Preprint. Discussion started: 1 April 2026

Bosse, J., Iden, S. C., Durner, W., Sut-Lohmann, M., and Peters, A.: Extending the measurement range of the simplified evaporation method using humidity sensors, Vadose Zone Journal, 24, https://doi.org/10.1002/vzj2.70015, 2025.

Diamantopoulos, E., Durner, W., Iden, S. C., Weller, U., and Vogel, H.-J.: Modeling dynamic non-equilibrium water flow observations under various boundary conditions, Journal of Hydrology, 529, 1851–1858, https://doi.org/10.1016/j.jhydrol.2015.07.032, 2015.

Diamantopoulos, E. and Durner, W.: Dynamic Nonequilibrium of Water Flow in Porous Media: A Review, Vadose Zone Journal, 11, vzj2011.0197, https://doi.org/10.2136/vzj2011.0197, 2012.

Diamantopoulos, E., Simunek, J., and Weber, T. K. D.: Implementation of the Brunswick model system into the Hydrus software suite, Vadose Zone Journal, 23, https://doi.org/10.1002/vzj2.20326, 2024.

Hassanizadeh, S. M., Celia, M. A., and Dahle, H. K.: Dynamic Effect in the Capillary Pressure–Saturation Relationship and its Impacts on Unsaturated Flow, Vadose Zone Journal, 1, 38–57, https://doi.org/10.2136/vzj2002.3800, 2002.

Hohenbrink, T. L., Jackisch, C., Durner, W., Germer, K., Iden, S. C., Kreiselmeier, J., Leuther, F., Metzger, J. C., Naseri, M., and Peters, A.: Soil water retention and hydraulic conductivity measured in a wide saturation range, Earth Syst. Sci. Data, 15, 4417–4432, https://doi.org/10.5194/essd-15-4417-2023, 2023.

Holbak, M., Abrahamsen, P., Hansen, S., and Diamantopoulos, E.: A Physically Based Model for Preferential Water Flow and Solute Transport in Drained Agricultural Fields, Water Resources Research, 57, https://doi.org/10.1029/2020WR027954, 2021.

Iden, S. C. and Durner, W.: Comment on “Simple consistent models for water retention and hydraulic conductivity in the complete moisture range” by A. Peters, Water Resources Research, 50, 7530–7534, https://doi.org/10.1002/2014WR015937, 2014.

Ippisch, O., Vogel, H.-J., and Bastian, P.: Validity limits for the van Genuchten–Mualem model and implications for parameter estimation and numerical simulation, Advances in Water Resources, 29, 1780–1789, https://doi.org/10.1016/j.advwatres.2005.12.011, 2006.

Jarvis, N., Koestel, J., and Larsbo, M.: Understanding Preferential Flow in the Vadose Zone: Recent Advances and Future Prospects, Vadose Zone Journal, 15, 1–11, https://doi.org/10.2136/vzj2016.09.0075, 2016.

Leij, F. J., Ghezzehei, T. A., and Or, D.: Modeling the dynamics of the soil pore-size distribution, Soil and Tillage Research, 64, 61–78, https://doi.org/10.1016/S0167-1987(01)00257-4, 2002.

Leuther, F. and Schlüter, S.: Impact of freeze–thaw cycles on soil structure and soil hydraulic properties, SOIL, 7, 179–191, https://doi.org/10.5194/soil-7-179-2021, 2021.

METER Group GmbH: WP4C Manual, available at: https://metergroup.com/support/downloads-page/manuals/, 2025.

METER Group GmbH: Operation Manual KSAT, available at: https://metergroup.com/support/downloads-page/manuals/.

Meurer, K., Barron, J., Chenu, C., Coucheney, E., Fielding, M., Hallett, P., Herrmann, A. M., Keller, T., Koestel, J., Larsbo, M., Lewan, E., Or, D., Parsons, D., Parvin, N., Taylor, A., Vereecken, H., and Jarvis, N.: A framework for modelling

https://doi.org/10.5194/egusphere-2026-1405
Preprint. Discussion started: 1 April 2026

soil structure dynamics induced by biological activity, Global change biology, 26, 5382–5403, https://doi.org/10.1111/gcb.15289, 2020.

Munkholm, L. J., Heck, R. J., and Deen, B.: Long-term rotation and tillage effects on soil structure and crop yield, Soil and Tillage Research, 127, 85–91, https://doi.org/10.1016/j.still.2012.02.007, 2013.

Peters, A.: Simple consistent models for water retention and hydraulic conductivity in the complete moisture range, Water Resources Research, 49, 6765–6780, https://doi.org/10.1002/wrcr.20548, 2013.

Peters, A. and Durner, W.: Simplified evaporation method for determining soil hydraulic properties, Journal of Hydrology, 356, 147–162, https://doi.org/10.1016/j.jhydrol.2008.04.016, 2008.

Richards, L. A.: CAPILLARY CONDUCTION OF LIQUIDS THROUGH POROUS MEDIUMS, Physics, 1, 318–333, https://doi.org/10.1063/1.1745010, 1931.

Sarkar, S., Germer, K., Maity, R., and Durner, W.: Measuring near-saturated hydraulic conductivity of soils by quasi unit-gradient percolation—1. Theory and numerical analysis, J. Plant Nutr. Soil Sci., 182, 524–534, https://doi.org/10.1002/jpln.201800382, 2019a.

Sarkar, S., Germer, K., Maity, R., and Durner, W.: Measuring near-saturated hydraulic conductivity of soils by quasi unit-gradient percolation—2. Application of the methodology, J. Plant Nutr. Soil Sci., 182, 535–540, https://doi.org/10.1002/jpln.201800383, 2019b.

Schelle, H., Heise, L., Jänicke, K., and Durner, W.: Water retention characteristics of soils over the whole moisture range: a comparison of laboratory methods, European J Soil Science, 64, 814–821, https://doi.org/10.1111/ejss.12108, 2013.

Schindler, U., Durner, W., Unold, G. von, Mueller, L., and Wieland, R.: The evaporation method: Extending the measurement range of soil hydraulic properties using the air-entry pressure of the ceramic cup, J. Plant Nutr. Soil Sci., 173, 563–572, https://doi.org/10.1002/jpln.200900201, 2010.

Schlüter, S., Großmann, C., Diel, J., Wu, G.-M., Tischer, S., Deubel, A., and Rücknagel, J.: Long-term effects of conventional and reduced tillage on soil structure, soil ecological and soil hydraulic properties, Geoderma, 332, 10–19, https://doi.org/10.1016/j.geoderma.2018.07.001, 2018.

Topp, G. C., Klute, A., and Peters, D. B.: Comparison of Water Content-Pressure Head Data Obtained by Equilibrium, Steady-State, and Unsteady-State Methods, Soil Science Soc of Amer J, 31, 312–314, https://doi.org/10.2136/sssaj1967.03615995003100030009x, 1967.

USDA: Soil Taxonomy, 2nd Edn., 1999.

van Genuchten, M. T.: A Closed-form Equation for Predicting the Hydraulic Conductivity of Unsaturated Soils, Soil Science Soc of Amer J, 44, 892–898, https://doi.org/10.2136/sssaj1980.03615995004400050002x, 1980.

Vereecken, H., Schnepf, A., Hopmans, J. W., Javaux, M., Or, D., Roose, T., Vanderborght, J., Young, M. H., Amelung, W., Aitkenhead, M., Allison, S. D., Assouline, S., Baveye, P., Berli, M., Brüggemann, N., Finke, P., Flury, M., Gaiser, T., Govers, G., Ghezzehei, T., Hallett, P., Hendricks Franssen, H. J., Heppell, J., Horn, R., Huisman, J. A., Jacques, D., Jonard, F., Kollet, S., Lafolie, F., Lamorski, K., Leitner, D., McBratney, A., Minasny, B., Montzka, C., Nowak, W.,

https://doi.org/10.5194/egusphere-2026-1405
Preprint. Discussion started: 1 April 2026

Pachepsky, Y., Padarian, J., Romano, N., Roth, K., Rothfuss, Y., Rowe, E. C., Schwen, A., Šimůnek, J., Tiktak, A., van Dam, J., van der Zee, S., Vogel, H. J., Vrugt, J. A., Wöhling, T., and Young, I. M.: Modeling Soil Processes: Review, Key Challenges, and New Perspectives, Vadose Zone Journal, 15, 1–57, https://doi.org/10.2136/vzj2015.09.0131, 2016.

Vogel, H.-J., Gerke, H. H., Mietrach, R., Zahl, R., and Wöhling, T.: Soil hydraulic conductivity in the state of nonequilibrium, Vadose Zone Journal, 22, https://doi.org/10.1002/vzj2.20238, 2023.

Weber, T. K. D., Weihermüller, L., Nemes, A., Bechtold, M., Degré, A., Diamantopoulos, E., Fatichi, S., Filipović, V., Gupta, S., Hohenbrink, T. L., Hirmas, D. R., Jackisch, C., van Jong Lier, Q. de, Koestel, J., Lehmann, P., Marthews, T. R., Minasny, B., Pagel, H., van der Ploeg, M., Shojaeezadeh, S. A., Svane, S. F., Szabó, B., Vereecken, H., Verhoef, A., Young, M., Zeng, Y., Zhang, Y., and Bonetti, S.: Hydro-pedotransfer functions: a roadmap for future development, Hydrol. Earth Syst. Sci., 28, 3391–3433, https://doi.org/10.5194/hess-28-3391-2024, 2024.

Weller, U. and Vogel, H.-J.: Conductivity and Hydraulic Nonequilibrium across Drainage and Infiltration Fronts, Vadose Zone Journal, 11, vzj2011.0134, https://doi.org/10.2136/vzj2011.0134, 2012.

Weller, U., Ippisch, O., Köhne, M., and Vogel, H.-J.: Direct Measurement of Unsaturated Conductivity including Hydraulic Nonequilibrium and Hysteresis, Vadose Zone Journal, 10, 654–661, https://doi.org/10.2136/vzj2010.0074, 2011.

Wind, G. P.: Capillary conductivity data estimated by a simple method: In: Rijtema, P.E., Wassink, H. (Eds.), Water in the Unsaturated Zone, vol. 1. Proceedings of the Wageningen Symposium, 19–23 June 1966. Int. Assoc. Sci. Hydrol. Publ. (IASH), Gentbrugge, The Netherlands and UNESCO, Paris., 1968.

Zhang, Z., Liu, K., Zhou, H., Lin, H., Li, D., and Peng, X.: Three dimensional characteristics of biopores and non-biopores in the subsoil respond differently to land use and fertilization, Plant Soil, 428, 453–467, https://doi.org/10.1007/s11104-018-3689-3, 2018.